Current Research in Food Science 5 (2022) 479–490

Contents lists available at ScienceDirect

Current Research in Food Science

journal homepage: www.sciencedirect.com/journal/current-research-in-food-science

Vibrational and fluorescence spectroscopy to study gluten and zein interactions in complex dough systems

Azin Sadat [a], Maria G. Corradini [a,b], Iris J. Joye [a,*]

[a] Department of Food Science, University of Guelph, Guelph, Canada
[b] Arrell Food Institute, University of Guelph, Guelph, Canada

ARTICLE INFO

Keywords:
Gluten
Zein
Amide I band
Spectroscopy
Disulfide bridges
Aromatic amino acids

ABSTRACT

The volume-spanning network formed by gluten during breadmaking is crucial in the production of high-quality bakery products. Zein proteins are also capable of forming a protein network under specific conditions. Vibrational (Fourier transform infrared spectroscopy (FTIR) and Raman scattering) and fluorescence spectroscopy are powerful, non-invasive techniques capable of assessing protein structures and interactions. The main objective of this project was to explore the suitability of these techniques to study zein and gluten structures and interactions in complex dough systems. The dough samples were prepared by mixing 20 w/w% of protein (with different proportions of zein and gluten) and 80 w/w% of corn starch. The tyrosine (Tyr) fluorescence emission peak (λ_{exc} = 280 nm) was still present even in those zein-gluten samples containing the highest gluten concentration and lowest zein concentration. This suggests that the Tyr moieties (stemming from zein) are not in close proximity to tryptophan (Trp) of gluten and their fluorescence is not quenched efficiently. Raman scattering results also showed the presence of different Tyr residues, exposed and buried, as well as different conformations of disulfide bridges, in zein and gluten samples. Based on the results from spectroscopic measurements and scanning electron microscopy (SEM), two distinct network structures composed of gluten and zein were identified in the mixed dough systems. The present work illustrates how complementary vibrational (Raman scattering and FTIR) and fluorescence spectroscopy methods can be combined to non-invasively assess protein structure and interactions in a complex food matrix.

1. Introduction

Gluten proteins are generally classified into 'monomeric' gliadins and 'polymeric' glutenins. They are known for their ability to form a viscoelastic dough required for the production of high-quality bakery products (Delcour et al., 2012). Zein is the main protein in corn, comprising about 50% of the total endosperm proteins (Delcour and Hoseney, 2010). While the glass transition temperature (T_g) of gluten is below room temperature (23 °C) at moisture contents above 16% (Hoseney, 1986), the T_g of zein is above room temperature at moisture contents of 28% and higher (Lawton, 1992). By increasing the temperature above zein's T_g (28 °C at >20% moisture content), its propensity for aggregation and cross-linking is enhanced, and it eventually can form a continuous protein network (Delcour and Hoseney, 2010).

Zein-based viscoelastic dough systems have been extensively studied during the past few years (Andersson et al., 2011; Erickson et al., 2012; Johansson et al., 2012; Mejia et al., 2007; Smith et al., 2014). The study of cereal dough systems in their "natural state" is difficult due to their inherent high complexity and the limited number of analytical techniques that do not require extensive sample preparation. Hence, developing and further optimizing non-invasive techniques such as vibrational and luminescence spectroscopy is crucial to monitor zein and gluten interactions and structure, and describe their effects on dough properties and stability (Sadat et al., 2019).

Fourier-transformed Infrared Spectroscopy (FTIR) has been used to probe the gluten secondary structure in dough as a function of dough composition (e.g., the addition of chemicals and enzymes during dough preparation (Bagagli et al., 2014), supplementation with bran and dietary fibre (Bock et al., 2013; Bock and Damodaran, 2013; Nawrocka et al., 2016)), processing conditions and parameters (e.g., mixing/mechanical deformation (Wellner et al., 2005)), and different levels of gluten hydration (Belton et al., 1995). Similarly, FTIR has also been used to understand the changes in the secondary structure of zein in different solvents (Argos et al., 1982; Y. Chen et al., 2014), gain insights

* Corresponding author.
E-mail address: ijoye@uoguelph.ca (I.J. Joye).

https://doi.org/10.1016/j.crfs.2022.02.009
Received 3 November 2021; Received in revised form 15 February 2022; Accepted 18 February 2022
Available online 25 February 2022

into bond formation between zein and other molecules (Chen and Subirade, 2009; Wheelwright et al., 2013; Zhang et al., 2010), and characterize zein dough systems (King et al., 2016; Mejia et al., 2007; Sly et al., 2014). Federici et al. (2021) also used FTIR to investigate the effect of thermal treatment on zein-starch doughs. They observed the development of fibrous protein structure in doughs with thermally treated zein that was attributed to an increase in β-sheet secondary structure.

Intrinsic protein fluorescence spectroscopy provides information about the chemical and physical environment of aromatic amino acids (Trp and Tyr) present in the samples and has previously been used to study gluten conformation in cereal systems (Andersen and Mortensen, 2008; Bonomi et al., 2004; Kokawa et al., 2011). To the best of our knowledge, fluorescence spectroscopy has not yet been used to assess zein's viscoelastic state, while it can provide useful information about the aromatic amino acids' side-chain environment of zein in its viscoelastic state. Raman spectroscopy is a powerful tool that has been used to study the different components of dough and wheat kernels (Cebi et al., 2017; Piot et al., 2001). There are only a limited number of studies on zein and zein-based materials using Raman spectroscopy. The studied systems include zein-chitosan films (Escamilla-García et al., 2013), zein nanoparticles (Hu et al., 2015; Y. Wang et al., 2013), and zein fibres and films (Alhusein et al., 2013; Escamilla-García et al., 2013; Federici et al., 2020; Fernandez et al., 2009). This technique can also provide useful information about the different conformations of disulfide bonds in protein samples (Zhou et al., 2014). Despite the numerous studies available on gluten and zein dough (Andersson et al., 2011; Bache and Donald, 1998; Jazaeri et al., 2015; Khuzwayo et al., 2020; Kokawa et al., 2011; Rumińska et al., 2020; Schober et al., 2008, 2010; Sly et al., 2014), only a very limited number of them have reported on gluten-zein interactions in a gluten-zein dough system. In addition, none of them have used the above-described non-invasive techniques to study these proteins in their 'natural,' undisturbed state in a mixed system. Bugusu et al. (2001) investigated the effect of the addition of zein (1, 5, and 10%) to sorghum-wheat composite flour (20% sorghum) on the rheological properties of the dough and its breadmaking quality. They observed an increase in dough extensibility and specific bread volume with increasing amounts of zein. This was attributed to zein's effect on the gluten network's strength and its ability to retain CO_2. However, it was not clear whether these improvements resulted from the interaction of zein with gluten or the effect of zein alone. Bugusu et al. (2002) studied the microstructure of zein and wheat gluten in composite dough and bread systems using confocal laser scanning microscopy (CLSM). They observed an outer layer of loose, thin zein fibrils coating the gluten network, leading to enhanced resistance to gas cell rupture. They stated that zein fibrils form a finer network than gluten, which is mainly external to the gluten network.

The interactions and structure of zein and gluten networks are difficult to study as most analytical methods usually require the extraction or isolation of the proteins, which inherently changes the characteristics of these systems and leaves researchers with the uncertainty of having introduced artifacts during sample preparation. Vibrational spectroscopy, which comprises both infrared absorption and Raman scattering, and fluorescence spectroscopy are non-invasive methods, that do not require isolation or extensive sample preparation, and use only small amounts of sample. Therefore, the main objective of this project was assessing the feasibility of these non-invasive methods to study complex zein-gluten dough systems.

2. Materials and methods

2.1. Sample preparation

Zein from maize was obtained from Flo Chemical Corp (Ashburnham, MA, USA), while commercial gluten flour and corn starch were purchased from a local market (BulkBarn, Canada). The protein content of zein powder and gluten flour were 87.1% and 72.6% db (Dumas method, N × 6.25 and N × 5.8), respectively. Dough samples were prepared by mixing 80 w/w% of corn starch with 20 w/w% of protein. Different ratios of zein and gluten (w/w) (zein:gluten, 0:20, 15:5, 10:10, 5:15, 20:0) made up this protein fraction. The moisture content of the corn starch, gluten flour, and zein were 10.62%, 7.06%, and 4.96%, respectively. All the ingredients were kept at 40 °C overnight in separate glass jars before mixing to ensure they were equilibrated to a temperature exceeding the T_g of zein before using them. The mixer and the mixing bowl were also placed at 40 °C overnight, so the ingredients' temperature didn't drop during mixing. 100 g of the dry ingredients were then dry-mixed into a homogenous powder in the mixing bowl prior to adding 75 g of Milli-Q water. The dough was prepared using a 100 g micro mixer (National MFG. Co., Lincoln, Canada) at 40 °C and 25% relative humidity (RH). All samples were mixed for 5 min prior to further analysis. Images of the prepared dough samples can be found in supplementary data (Fig. S1).

2.2. Attenuated total reflectance (ATR) FTIR spectroscopy

A Vertex 70 series spectrophotometer (Bruker Optics, Billerica, MA, USA) was used to study the secondary structure of the protein fraction in dough samples. This spectrometer is equipped with a horizontal multi-reflectance ZnSe crystal accessory. The instrument houses a deuterated triglycine sulfate (DTgS) detector and a KBr beam splitter. The spectra of dough samples were collected in the 800-3500 cm^{-1} region at room temperature using 4 cm^{-1} resolution, an aperture diameter of 6 mm, and 32 scans. To minimize the presence of water vapor in the system, the internal humidity of the instrument was brought to ~zero by refreshing the desiccants the night before measurement and purging the system with N_2 gas during the measurement. The FTIR spectra of the dough samples (sample measurement) and continuous phase (reference measurement; Milli-Q water) were collected at least in triplicate. All the recorded spectra were subjected to a two-step normalization process involving a vector and offset normalization (Sadat and Joye, 2020). The FTIR spectra shown in this article are background corrected and normalized. The averaged normalized reference spectrum (Milli-Q water) was then subtracted from each normalized sample measurement. OPUS software (Bruker Optics, Billerica, MA, USA) was used for spectra acquisition, normalization, and subtraction of the reference spectrum (Sadat and Joye, 2020).

The water-corrected spectra of dough samples were then analyzed using OriginPro 2020 (OriginLab Corporation, Northampton, MA, USA). The amide I band was subjected to curve fitting based on the second derivative hidden peak analysis according to the method described by Sadat and Joye (2020). The respective peaks were characterized by the Voigt function. The residual errors of the fits were less than 2×10^{-4} and randomly distributed in all cases. The relative peak areas of the absorbance bands of each secondary structure are presented as the "percentage of the area of the fitted region."

2.3. Steady-state fluorescence spectroscopy measurements

Front-face fluorescence spectra were recorded at 40 °C using triangular quartz cuvettes in a Fluoromax 4 Spectrofluorometer (Horiba Scientific Inc., Edison, NJ, USA). The spectra for intrinsic luminescent aromatic amino acids, Tyr and Trp, were collected upon excitation at 280 nm (λ_{exc}) over a wavelength range from 290 to 425 nm (λ_{em}). Trp fluorescence intensity was also recorded using an excitation wavelength of 295 nm over emission wavelengths from 300 to 425 nm. Excitation and emission slit widths were set at 1.5 and 3.0 nm, respectively. The measurements were all performed in triplicate. The water spectrum (blank) was subtracted from the spectra of the dough samples to remove the cuvettes background. The water-subtracted spectra were subsequently normalized. To separate the contributions of Tyr and Trp to the overall emission obtained at 280 nm, the data were subjected to a

deconvolution procedure using OriginPro 2020 (OriginLab Corporation, Northampton, MA, USA). The respective peaks were characterized with a lognormal distribution function.

To further characterize the β-sheet enriched fibrils formed in dough samples, the spectra of dough samples were also collected at an excitation wavelength of 350 nm over an emission wavelength range from 370 to 550 nm. For all the measurements, the excitation and emission slit widths were set at 1 and 2 nm, respectively.

2.4. Thioflavin T fluorescence assay

Thioflavin T (ThT) (Fisher Scientific, Canada) is a cationic benzothiazole dye that becomes highly fluorescent by interacting with β-sheet rich matrices (Farrokhi et al., 2019; Sen et al., 2009). This fluorophore behaves as a molecular rotor and has been extensively used to detect β-sheet rich amyloid fibrils in medical applications. In this study, ThT fluorescence intensity was monitored to assess the extent of the β-sheet structures, the potential formation of fibrils and the stiffening of the matrix in the studied dough samples. For this purpose, a ThT solution (0.64 mM) was prepared and kept at 40 °C overnight prior to mixing with corn starch and gluten or/and zein following the same process described in the *sample preparation* section (2.1). To avoid inner filter effects, the ThT concentration vs. emission intensity relationship was mapped over a wide range of concentrations (0.08–0.66 mM), and the 0.64 Mm concentration which was within the linear region of the intensity vs. concentration relationship, was selected for further studies. The fluorescence emission spectra of dough samples containing ThT were then recorded at a 440 nm excitation wavelength over an emission wavelength range from 460 to 550 nm. Both the excitation and emission slits were set at 1.5 nm. The measurements were performed at 40 °C using triangular quartz cuvettes. The spectrum of water (blank) was subtracted from the fluorescence spectra of dough samples to remove the cuvettes background. The resultant spectra were subsequently normalized to the maximum.

2.5. FT-Raman spectra collection and data analysis

The FT-Raman spectra of dough samples were recorded using a Bruker FRA 106/s module (Billerica, Massachusetts, USA) on a Bruker IFS66vs FT-Raman spectrometer (Billerica, Massachusetts, USA) with excitation at 1064 nm and 2 cm^{-1} resolution using a 180° backscattering geometry. A total of 4000 scans were recorded between 400 and 3500 cm^{-1} using a laser power of 525 mW. Dough samples were packed in a standard 2 mm cavity cell. The baseline correction was performed with a 5 point Savitsky-Golay function. The baseline-corrected spectra were then normalized against the starch band at 477 cm^{-1}. The disulfide bridge region (490-550 cm^{-1}), aromatic amino acids regions (Tyr doublet band [I_{850}/I_{830}]), and amide I band (1590-1700 cm^{-1}) were analyzed. To determine changes in the Tyr doublet band intensity and the conformation of disulfide bridges, difference spectra were calculated since the Raman spectrum of starch shows a distinct band within these spectral regions. The difference spectra were obtained by subtracting the normalized starch spectrum from that of the dough samples. The disulfide bridge region (490-550 cm^{-1}) was analyzed according to the method described by Pfeuti et al. (2019) to detect and quantify the percentage distribution of the SS bond conformations [gauche-gauche-gauche ($SS_{g\text{-}g\text{-}g}$, g-g-g), trans-gauche-gauche ($SS_{t\text{-}g\text{-}g}$, t-g-g), and trans-gauche-trans ($SS_{t\text{-}g\text{-}t}$, t-g-t)]. The peak shapes were approximated by a Gaussian function. The fitting deconvolution procedure was also conducted on the amide I band to calculate the relative amounts of each secondary structure as described by Sadat and Joye (2020). All the data analysis procedures were performed using OriginPro 2020 (OriginLab Corporation, Northampton, MA, USA). The FT-Raman measurements were performed in duplicate.

2.6. Cryo scanning electron microscopy (Cryo-SEM)

A scanning electron microscope (FEI Quanta FEG 250) was used to visualize the dough structure at the Molecular and Cellular Imaging Facility of the University of Guelph. The prepared dough samples were immediately mounted on stubs at 40 °C after mixing. No glue was used to fix the dough to the stub. The shuttle with the stub and sample was immersed in a liquid nitrogen slurry immediately after mounting to quickly freeze the material. The shuttle was then transferred to the aQuilo chamber while maintaining a low vacuum. Fracture was performed with the top knife. Sublimation was carried out at −90 °C for 10 min, while the sputtering used argon to generate a layer of ~35 nm of platinum (10 mA for 90 s) onto the fractured-sublimed-sample. A Quorum PP3010 Cryo-Unit was used to freeze, fracture, sublime, and sputter coat the sample before its insertion into the vacuum chamber of the SEM. A low temperature of −175 °C on the sample holder was maintained while acquiring the images. Images were captured using 20 kV at 1000x, 5000x, and 10,000× magnification with the software provided by the manufacturer.

2.7. Size-exclusion high-performance liquid chromatography (SE-HPLC)

SE-HPLC was conducted according to the method described by Rombouts et al. (2014) to compare the extractability and molecular size distribution of proteins from different dough samples. For this purpose, 10 mg of freeze-dried dough sample was extracted with 1.0 mL of 50 mM sodium phosphate buffer (pH 6.8) containing 2.0% (w/v) SDS. To determine protein extractability under reducing conditions, samples were extracted with 1.0 mL SDS buffer to which 2.0 M urea and 1.0 (w/v) % DTT were added. The suspensions were vortexed and shaken at 150 rpm for 60 min at room temperature and under nitrogen atmosphere. They were then centrifuged for 10 min at 10,000 *g* and the supernatant was filtered through a 0.45 μm syringe filter. The protein extracts were analyzed with a HPLC system (Shimadzu, Kyoto, Japan) using a Biosep-SEC-S4000 column with a separation range from 15 to 500 kDa (300 mm × 7.8 mm, Phenomenex, Torrance, CA, USA). The SDS buffer was used as mobile phase at a flow rate of 1.0 mL/min at 30 °C. 20 μL of sample was injected in the HPLC system and protein elution was monitored by measuring the absorbance at 214 nm with a SPD-10A UV-VIS detector.

2.8. Syneresis measurement

The dough samples were placed in centrifuge tubes and centrifuged at 500 *g* for 3 min at room temperature, using a Beckman Coulter Allegra X-15R Centrifuge (Beckman Coulter Co., IN, USA). The free water was poured off and weighed. The extent of syneresis (%) was defined as the percentage of the liquid (w/w) separated from the dough network. The measurements were done in duplicate.

2.9. Statistical analysis

All measurements were performed in triplicate unless mentioned otherwise. The results are reported as mean values and standard deviations. The data were subjected to one-way ANOVA analysis, followed by Tukey's HSD testing. Differences were considered significant at a significance level of $p < 0.05$.

3. Results

3.1. FTIR and FT-Raman analysis of zein-gluten dough samples

3.1.1. Changes in secondary structure (amide I band)

The infrared and Raman scattering spectra of dough samples prepared with different ratios of gluten and zein were investigated. For FTIR spectra of dough samples, a wider range (1500-1700 cm^{-1}) has

been subjected to peak fitting to do a proper baseline correction. However, only the amide I band was used to characterize the secondary structure of the proteins due to its higher protein conformational sensitivity compared with amide II (Sadat and Joye, 2020). The second derivative of the FTIR and FT-Raman spectra was used as a peak sharpening method to identify the hidden peaks in the amide I region (Fig. 1 and Fig. 2). Peak fitting was applied to the original spectra to calculate the relative amount of each secondary structure (Table 1) from the area under the identified peaks. The FT-Raman band at around 1602 cm^{-1} (Fig. 2) which appeared in all dough samples is due to aromatic side chains of amino acids (Piccirilli et al., 2015). This band was not included in the quantitative analysis of the FT-Raman results.

The second derivative FTIR spectra (Fig. 1) of all dough samples showed a band at 1653 cm^{-1} assigned to the α-helix structure according to Sadat and Joye (2020). The second derivative FT-Raman spectra of dough samples showed α-helical bands between 1650 and 1660 cm^{-1} (Nawrocka et al., 2017). The FTIR and FT-Raman analysis of the 20:0 gluten:zein dough sample showed 41 ± 3% and 35 ± 1% of the α-helical structure, respectively (Table 1). This is consistent with previous reports (Nawrocka et al., 2016a,b,c; Zhou et al., 2014), indicating that a significant amount of gluten proteins in dough exhibit α-helical conformation. The β-turn structure was visible as one IR band at 1672 cm^{-1} (Sadat and Joye, 2020) and Raman bands between 1663 and 1674 cm^{-1} (Nawrocka et al., 2017; Rumińska et al., 2020) in all dough samples (Figs. 1 and 2). No random coil structure was observed in any of the dough samples in both FTIR and FT-Raman spectra. It has been stated that random coil content decreases with increasing hydrogen bonding interactions between proteins and a higher degree of inter- and intramolecular β-sheets (Chen et al., 2014; Prestrelski et al., 1993). This is in line with the high content of β-sheet structures observed in all dough samples (Table 1).

β-sheet structures were indeed the most prevalent secondary structures in all gluten and zein dough samples, based on both FTIR and FT-Raman measurements (Table 1). Two IR bands at 1616 and 1626 cm^{-1}, and one IR band at 1636 cm^{-1} were observed, which were previously assigned to intermolecular and intramolecular β-sheets, respectively (Piccirilli et al., 2015). Interestingly, the second derivative FTIR spectrum of the 0:20 gluten:zein sample showed a more prominent intramolecular β-sheet peak at 1636 cm^{-1} (~53 ± 8% of the β-sheet content) than the 20:0 gluten:zein sample, which had a more significant ($p < 0.05$, Fig. S2) contribution of intermolecular β-sheets (~74 ± 5% of the β-sheet content) (Fig. 1, Table 1). In addition, there was an overall decrease in the intermolecular β-sheet content in samples with increasing zein content (Table 1).

It has been demonstrated that parallel and antiparallel β-sheets can also be distinguished by FTIR spectroscopy. The band at ~1636 cm^{-1} has previously been assigned to both parallel and antiparallel β-sheets. However, the presence of antiparallel β-sheets has been associated with an additional high-frequency component between ~1685 and 1695 cm^{-1} (Cerf et al., 2009). The second derivative FTIR spectra of all dough samples showed two peaks located at 1636 and 1684 cm^{-1} which can be assigned to intramolecular antiparallel β-sheets (Fig. 1). The FT-Raman spectra of dough samples also showed the presence of three bands at 1676-1696 cm^{-1} assigned to antiparallel β-sheets (Fig. 2), according to literature (Nawrocka et al., 2016, 2017). These bands can indicate the formation of hydrogen bonds within gluten and zein proteins, mostly in the form of antiparallel β-sheets.

3.1.2. Changes in disulfide bridge conformations

The disulfide SS stretch bond appears in the 490-550 cm^{-1} region of the Raman spectra. It provides information about the structural/conformational changes in disulfide bridges (Zhou et al., 2014). Three different conformations can be found depending on the different conformational states of C–S–S–C atoms, *i.e.,* $SS_{g\text{-}g\text{-}g}$ (496-513 cm^{-1}), $SS_{t\text{-}g\text{-}g}$ (514-527 cm^{-1}), and $SS_{t\text{-}g\text{-}t}$ (527-548 cm^{-1}) (Pfeuti et al., 2019). Table 2 summarizes the results obtained from the deconvolution focusing on the disulfide bridges in the zein-gluten dough samples. Fitted spectra of the SS bond spectral region (490-550 cm^{-1}) and the band profile of the Gaussian components of the SS region for all dough samples are presented in the supplementary data (Figs. S3a–e). The conformational analysis of the disulfide bridges detected in spectra of 20:0 gluten:zein dough samples showed seven bands. These were located at 496, 501, and 508 cm^{-1} ($SS_{g\text{-}g\text{-}g}$), 516, and 522 cm^{-1} ($SS_{t\text{-}g\text{-}g}$), and 528 and 534 cm^{-1} ($SS_{t\text{-}g\text{-}t}$). The proportions of the g-g-g, t-g-g, and t-g-t conformations for the 20:0 gluten:zein samples were 41 ± 0, 36 ± 0, and 23 ± 1%, respectively. Similar results have been previously reported for wheat gluten (Nawrocka et al., 2015, 2016), indicating the prominent contribution of g-g-g and t-g-g in disulfide bridge conformation in gluten proteins. As shown in Table 2, the addition of zein caused a significant ($p < 0.05$, Fig. S4) decrease in the number of SS bonds in the g-g-g conformation while the number of disulfide bridges in the t-g-t conformation increased. The 0:20 gluten:zein dough sample contained 26 ± 5, 33 ± 6, and 41 ± 1% of disulfide bridges in g-g-g, t-g-g, and t-g-t conformation, respectively. The band at around 515 cm^{-1} is assigned to the formation of intrachain disulfide bonds (in t-g-g conformation) (Ferrer et al., 2011) and was present in all dough samples. The disappearance of this band has been attributed to intrachain disulfide bonds cleavage (Nawrocka et al., 2016a,b,c). This effect was not observed in any of the dough samples in this study.

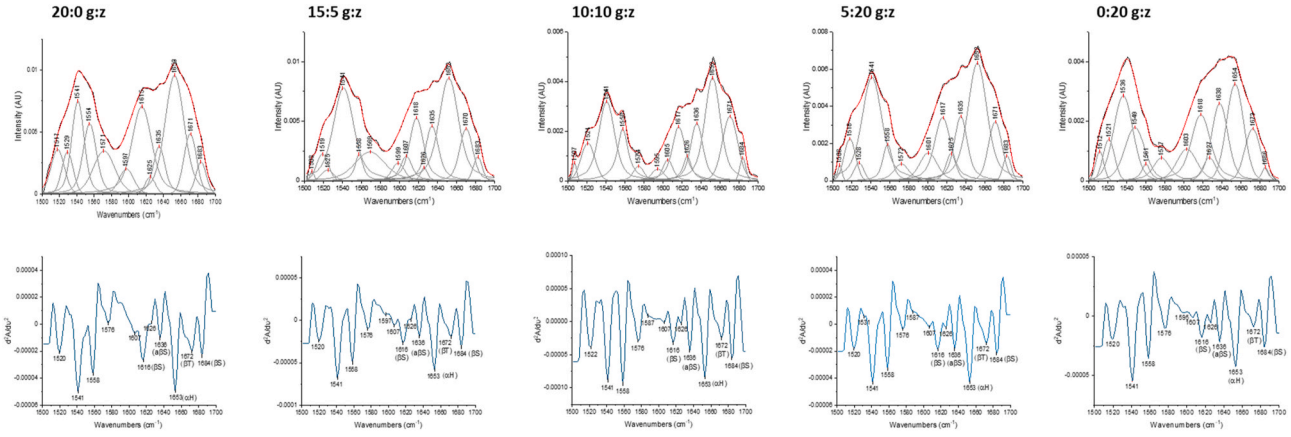

Fig. 1. Deconvoluted amide I bands (1600-1700 cm^{-1}) and their second derivatives of FTIR spectra of gluten/zein dough samples (g:z stands for gluten:zein proportions). Band assignments are based on Piccirilli et al. (2015), Nawrocka et al. (2017), Rumińska et al. (2020), Nawrocka et al. (2016a,b,c), and Zhou et al. (2014) studies.

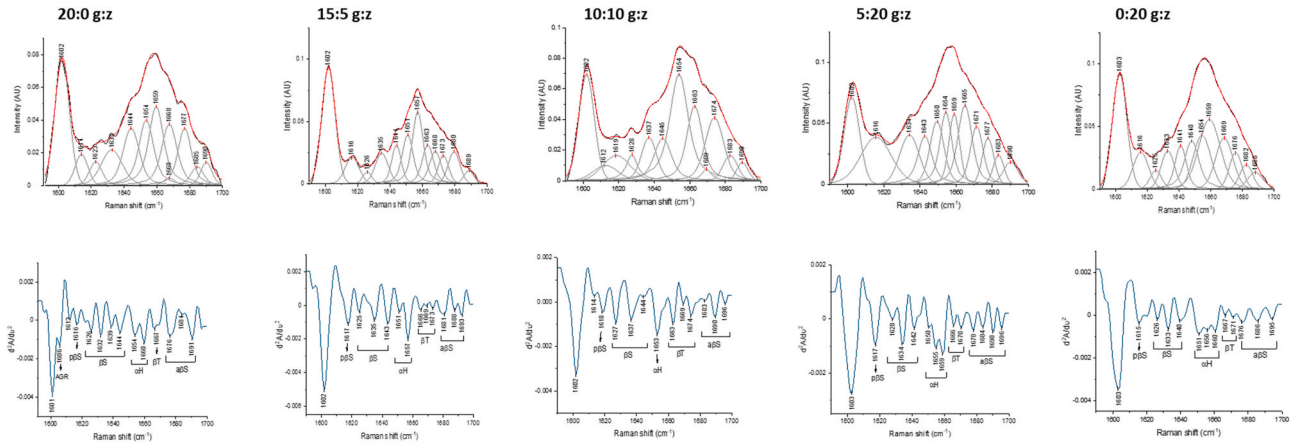

Fig. 2. Deconvoluted amide I bands (1600-1700 cm^{-1}) and their second derivatives of FT-Raman spectra of gluten/zein dough samples (g:z stands for gluten:zein proportions). Band assignments are based on Piccirilli et al. (2015), Nawrocka et al. (2017), Rumińska et al. (2020), Nawrocka et al. (2016a,b,c), and Zhou et al. (2014) studies.

Table 1
Relative amount of protein secondary structures in gluten/zein dough samples determined by peak fitting of the amide I in FTIR and FT-Raman spectra.

Dough samples Gluten:Zein	Secondary structures (%)						Method
	α-helix	β-sheet			β-turn	Random coil	
		Total	Intermolecular	Intramolecular			
20:0	41 ± 3	48 ± 2	74 ± 5	15 ± 5	11 ± 1	0	FTIR
	35 ± 1	58 ± 6			15 ± 1	0	FT-Raman
15:5	38 ± 2	46 ± 3	63 ± 1	26 ± 5	16 ± 2	0	FTIR
	33 ± 7	42 ± 1			30 ± 1	0	FT-Raman
10:10	38 ± 1	44 ± 1	53 ± 4	41 ± 4	18 ± 2	0	FTIR
	31 ± 4	39 ± 1			28 ± 7	0	FT-Raman
5:15	42 ± 0	44 ± 0	56 ± 1	38 ± 1	14 ± 0	0	FTIR
	38 ± 11	47 ± 1			20 ± 3	0	FT-Raman
0:20	32 ± 4	57 ± 2	40 ± 7	53 ± 8	11 ± 1	0	FTIR
	36 ± 3	56 ± 0			12 ± 3	0	FT-Raman

The analysis of variance of these data are available in supplementary file (Fig. S2).

Table 2
Proportion of disulfide bridge conformations (gauche-gauche-gauche ($SS_{g\text{-}g\text{-}g}$), trans-gauche-gauche ($SS_{t\text{-}g\text{-}g}$), and trans-gauche-trans ($SS_{t\text{-}g\text{-}t}$) in percentage and analysis of aromatic amino acid environment- Tyr (I_{850}/I_{830}- of the FT-Raman spectra for zein and gluten dough samples.

Gluten:Zein proportion	Peak max. ($SS_{g\text{-}g\text{-}g}$) (cm^{-1})	$SS_{g\text{-}g\text{-}g}$ (%)	Peak max. ($SS_{t\text{-}g\text{-}g}$) (cm^{-1})	$SS_{t\text{-}g\text{-}g}$ (%)	Peak max. ($SS_{t\text{-}g\text{-}t}$) (cm^{-1})	$SS_{t\text{-}g\text{-}t}$ (%)	I_{850}/I_{830}
20:0	496, 501, 508	41 ± 0	516, 522	36 ± 0	528, 534	23 ± 1	1.43 ± 0.23
15:5	497, 504, 508	33 ± 3	516, 525	45 ± 0	529, 534, 540, 543	22 ± 2	0.92 ± 0.15
10:10	499, 504, 508	40 ± 1	515, 521, 524, 527,	38 ± 1	533, 540, 544	21 ± 3	0.52 ± 0.20
5:15	499, 504, 508	27 ± 0	515, 521	34 ± 4	528, 535, 543	39 ± 4	0.79 ± 0.16
0:20	500, 505, 510	26 ± 5	515, 522	33 ± 6	527, 534, 541, 548	41 ± 1	0.68 ± 0.06

The analysis of variance of these data are available in supplementary file (Fig. S4 and Fig. S6).

3.1.3. Changes in the Tyr environment

The Tyr doublet bands located at 830 and 850 cm^{-1} in the FT-Raman spectra are useful to monitor the microenvironment around Tyr residues. Tyr doublet bands arise from the Tyr ring vibration. The intensity ratio of the Tyr ring vibrations at 850 and 830 cm^{-1} (I_{850}/I_{830}) is proportional to the number of "exposed" vs. "buried" Tyr residues and holds information about the hydrogen bonding capacity of the phenol hydroxyl group (Yada and Jackman, 2012). If $I_{850}/I_{830} > 1$, the Tyr residues are most likely located on the surface of the protein network, and the phenolic OH will be simultaneously an acceptor and donor of moderate to weak hydrogen bonding. If $I_{850}/I_{830} < 1$, the Tyr residues are likely to be fully or partially buried inside the protein structure, and the phenolic hydroxyl is the proton donor in a strong hydrogen bond (Yada and Jackman, 2012). As shown in Table 2 and Fig. S5, the value of I_{850}/I_{830} for 20:0 gluten:zein dough sample was 1.43 ± 0.23%, similar to those calculated in previous studies (Ferrer et al., 2011; Nawrocka et al., 2015, 2016) for gluten proteins. The I_{850}/I_{830} value for the 0:20 gluten:zein sample (0.68 ± 0.06%), however, was significantly ($p < 0.05$, Fig. S6) smaller.

3.2. Fluorescence spectra analysis of zein or/and gluten dough samples

The fluorescence spectra of Trp in the zein-gluten dough samples obtained using front-face mode are presented in Fig. 3a. Increased zein content resulted in a progressive bathochromic shift of the Trp fluorescence maximum (Table S1). The Trp peak wavelength shifted from 351 nm in 20:0 gluten:zein to 365 nm in 5:15 gluten:zein dough samples (Table S1). The position of the peak maximum in Trp fluorescence can be

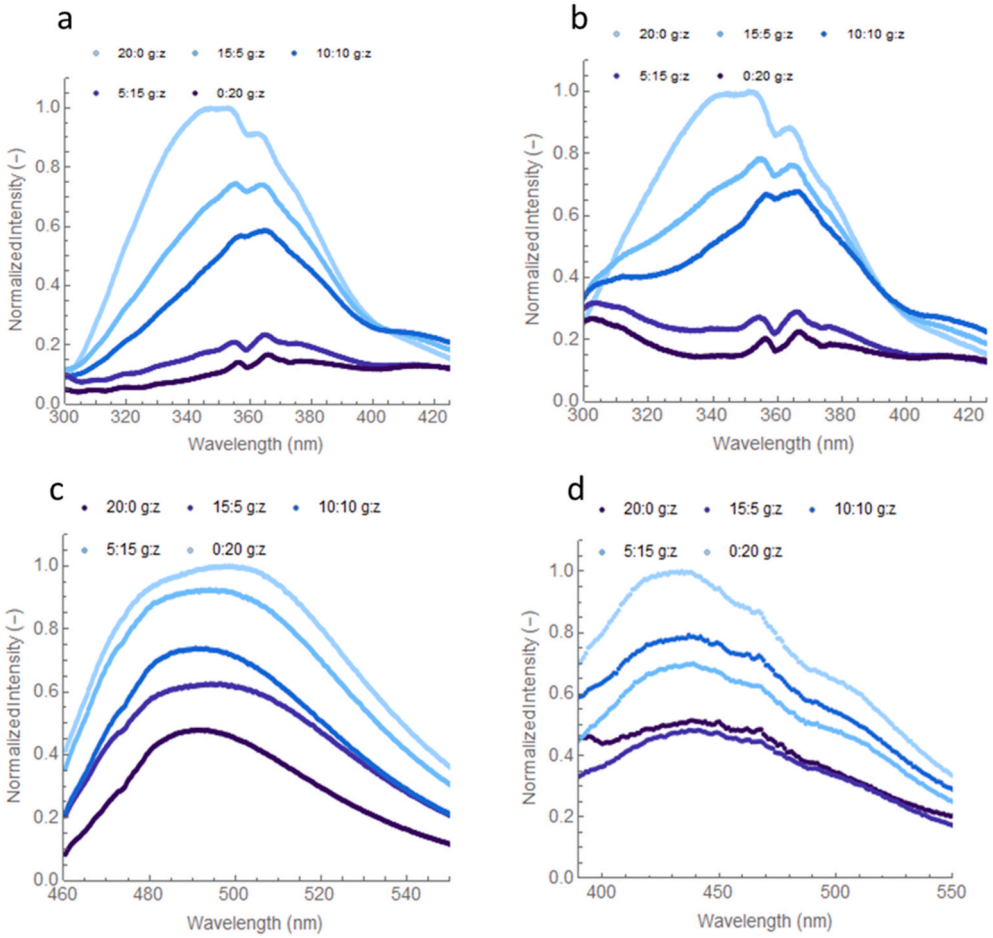

Fig. 3. (a) Fluorescence spectra of dough samples prepared with different proportions of zein and gluten (g:z stands for gluten:zein) excited at (a) 295 nm and (b) 280 nm (λ_{em} = 300–425 nm). (c) Fluorescence spectra of ThT in dough samples with different proportions of zein and gluten excited at 440 nm (λ_{em} = 460–550 nm). (d) Fluorescence spectra of dough samples prepared with different proportions of zein and gluten excited at 350 nm (λ_{em} = 390–550 nm).

related to the chemical environment of the Trp side chain (Fig. 4a), which will be further discussed in the *Discussion* section. The Trp peak intensity as a function of gluten concentration is presented in Fig. S7. As expected, the intensity of Trp (349–365 nm) increased at higher gluten concentrations at both excitation wavelengths (i.e., 280 & 295 nm), which is consistent with the fact that zein is deficient in Trp (Delcour and Hoseney, 2010). Thus, the Trp fluorescence emission originates solely from gluten proteins.

The emission spectrum of dough samples excited at 280 nm was also obtained to analyze both the Tyr and Trp residues contributions. As shown in Fig. 3b, the 20:0 gluten:zein emission spectrum exhibits one peak at around 350 nm, assigned to Trp, while the Tyr fluorescence signal (expected between 305 and 330 nm) is not detectable, most probably due to energy transfer between Tyr and Trp residues. Quenching of the Tyr fluorescence emission due to Förster resonance energy transfer (FRET) by nearby Trp allows assessing protein conformation and its changes during processes such as denaturation. FRET can occur between fluorophores that have overlapping excitation and emission spectra, as is the case between these amino acids. FRET only occurs when the two residues are within the Förster distance from each other, which is lower than 26 Å for Tyr and Trp (Fig. 4b) (Lakowicz, 2013). The fluorescence spectra of dough samples containing both gluten and zein exhibit a detectable Tyr peak (305–330 nm). The Tyr fluorescence emission, hence, is not as efficiently quenched by the Trp residues in these samples (Fig. 3b).

3.3. ThT fluorescence emission and fibril formation in zein or/and gluten dough samples

Previous studies have suggested that zein fibrillation is feasible and can be obtained under specific circumstances (e.g., changes of solvent polarity) (An et al., 2016; Erickson et al., 2012). ThT fluorescence emission has been used as an indicator of the presence of fibrils in systems with amyloid and non-amyloid forming proteins. The interaction of ThT with β-sheet rich structures was used as an indication for the occurrence of fibrillation in dough samples in this study (Biancalana and Koide, 2010). The β-sheet rich fibrils tend to be straight, unbranched, and ribbon-like fibrils with length of >1 μm and diameter of 10–20 nm (Biancalana and Koide, 2010; Krebs et al., 2005). They share a common internal structure called "cross β-sheets" consisting of laminated β-sheets (stabilized with H-bonds) whose strands are arranged perpendicular to the long axis of the fibrils (Krebs et al., 2005) (Fig. 4c). The surface of the cross-β-sheets forms the ThT-binding sites, which consists of channel-like motifs (Biancalana and Koide, 2010). As shown in Fig. 3c, the ThT fluorescence intensity progressively increased by adding zein to the dough system, possibly due to the formation of more β-sheet rich fibrils in samples with a higher amount of zein. This is in line with the FTIR secondary structure analysis showing an increase in β-sheet content with increasing proportion of zein in the dough samples (Table 1). Similar results have been obtained by Erickson et al. (2020a), who reported an increase in ThT fluorescence intensity at increasing β-sheet secondary structure percentages in zein-ethanol solutions. An et al. (2016) also observed an increase in ThT fluorescence intensity by

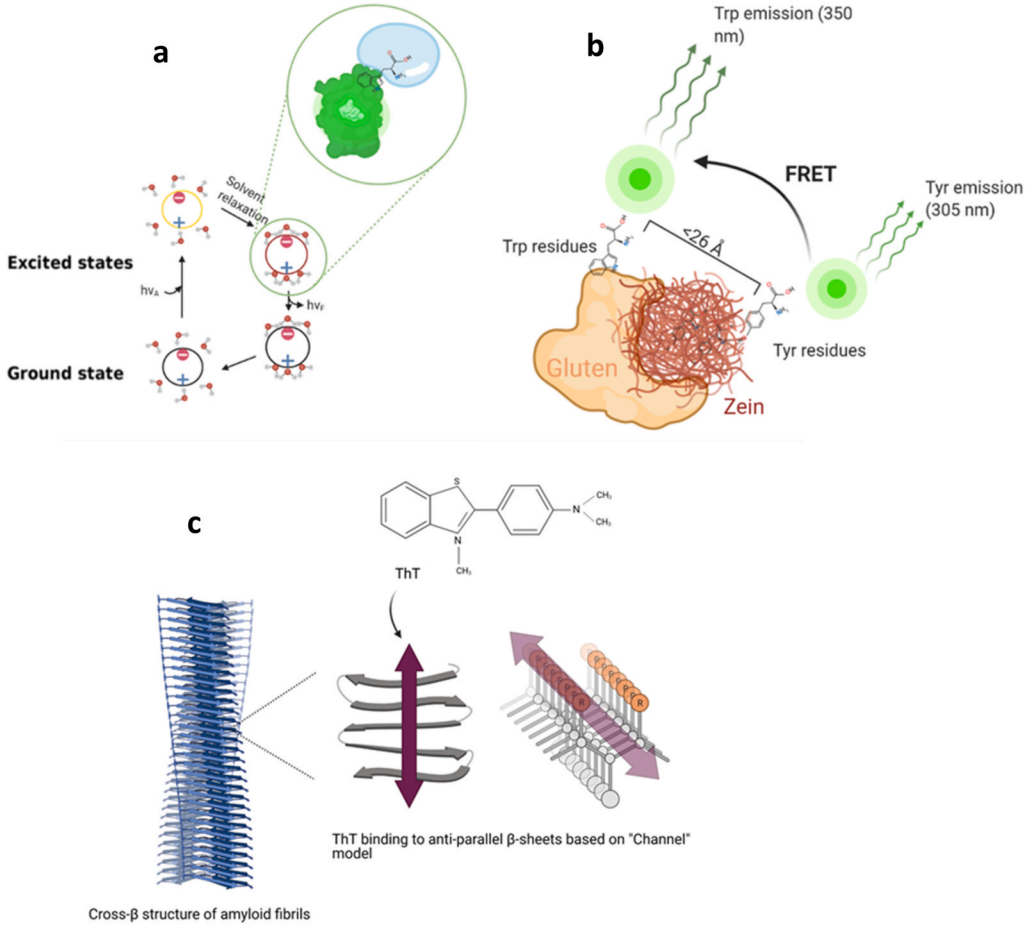

Fig. 4. (a) Graphical illustration of solvent effect on Trp residues (Adapted from Lakowicz (2013)). (b) Schematic representation of Förster Resonance Energy Transfer (FRET) from zein tyrosine (Tyr) residues to gluten tryptophan (Trp) residues. (c) Structure of Thioflavin T (ThT) and schematic diagram of protein fibrils-ThT interaction based on Biancalana and Koide (2010). (All graphics were created with BioRender).

fibrillation of α-zein upon thermal incubation. The 20:0 gluten:zein samples also presented a weak ThT fluorescence emission. It has been reported that gluten, to some extent, also forms protein fibrils (Delcour et al., 2012) which might be the reason for this observation.

Erickson et al. (2020) recently showed that the presence of non-fibril dense β-sheet structures could also lead to the observed increase in ThT emission intensity. However, the fluorescence emission of dough samples excited at 280 nm (Fig. 3b) shows the presence of a hump at around 425 nm, which has been previously attributed to the formation of highly structured β-sheet fibrils that promote proton channeling (Pinotsi et al., 2016). To further evaluate this peak, the different dough samples were excited at 350 nm (Fig. 3d). Interestingly, in all samples, an emission peak at around 420–440 nm was observed, which had a higher intensity in pure zein dough (0:20 gluten:zein) than that made with pure gluten (20:0 gluten:zein). This provides additional evidence of the formation of β-sheet rich fibrils that facilitate proton channeling, which will be further discussed in the *Discussion* section.

3.4. Microscopic analysis of zein or/and gluten dough samples

Fig. 5 shows representative images of the dough microstructures obtained with Cryo-SEM. SEM micrographs revealed the formation of two distinct networks in the pure zein and gluten dough systems (identified by arrows). In the gluten-only (i.e., 20:0 gluten:zein) dough sample (Fig. 5A-C), a continuous gluten network has been observed, which coats all the starch granules (white arrows). It can be seen that gluten proteins form a sheet-like structure that surrounds the starch granules. Similar observations have been reported before (Bache and Donald, 1998; Gao et al., 2017) for gluten dough samples. Upon the addition of zein to the gluten dough system, a new type of fibrillar network started to appear (Fig. 5D-F). As can be seen for the 10:10 gluten: zein dough samples (Fig. 5G-I), this fibrillar network (yellow arrows) coexists with the sheet-like gluten structure (white arrows) in the dough system. By increasing the zein concentration, these protein fibrils become wider in diameter (Fig. 5J-O) and are possibly responsible for the extensibility and viscoelastic behavior of zein dough (Lawton, 1992). The presence of protein fibrillar structures in the zein-starch dough has also been observed in previous studies (Bugusu et al., 2002; Lawton, 1992; Ncube et al., 2022). Bugusu et al. (2002) stated that zein proteins tend to form a finer network compared to that of gluten based on their CLSM measurements. This is in line with the observation for 15:5 gluten:zein (Fig. 5D-F) and 10:10 gluten:zein (Fig. 5G-I), indicating the presence of a thinner zein network compared with gluten. The ratio of zein and gluten in these samples is similar to those in the Bugusu et al.'s (2002) study. However, as shown in SEM micrographs for 0:20 gluten:zein (Fig. 5M-O), zein fibrils have lengths of >80 μm. This might suggest that the size of zein fibrils could be concentration-dependent, and they might form longer and wider fibrils at higher zein concentrations. Ncube et al. (2022) observed distinct fibrils with diameters varying between 20 and 500 μm in zein composite doughs. More measurements are needed to further support this assumption.

3.5. SE-HPLC analysis of dough samples

SE-HPLC provides information on the degree of covalent cross-linking in the dough system. As shown in Fig. 6a, the 20:0 gluten:zein

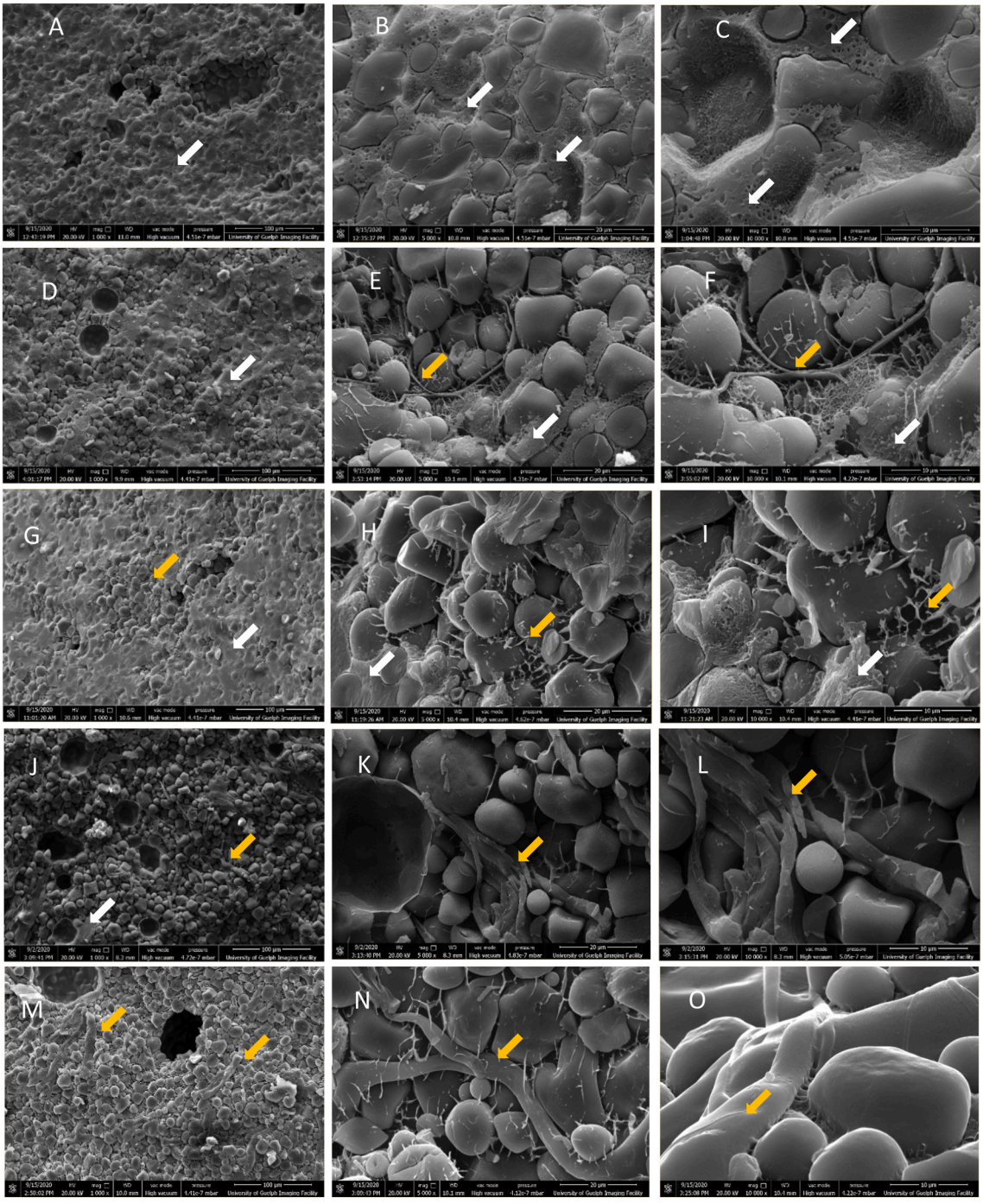

Fig. 5. SEM images of dough samples containing different ratios of gluten:zein; (A–C) 20:0 (D–F) 15:5 (G–I) 10:10 (J–L) 5:15 (M–O) 0:20. The white arrows point to the gluten protein network, and the orange arrows show the zein protein fibrils. (For interpretation of the references to colour in this figure legend, the reader is referred to the Web version of this article.)

sample showed the highest signal intensity in high molecular weight SDS-extracted fraction (F1). This HMW fraction is related to dough elasticity and strength (Cao et al., 2021) and its intensity decreased by increasing zein content (Fig. 6a). This is in line with the fact that gluten proteins contain the HMW glutenin polymers which are absent in the zein proteins. The fractions F3b, F4, and F5 would mainly consist of low molecular weight fractions including smaller gliadin monomers, zein monomers and some soluble proteins. Zein-containing samples seemed to have more of these low molecular weight fractions in the SDS-dough extract.

By addition of DTT and urea in the SDS extraction buffer, the disulfide bridges are reduced, and hydrogen bonds will be broken. Not surprisingly, a larger fraction of the proteins now eluted at later retention times as their molecular weight was significantly reduced. The reducing effect of DTT completely annihilated the fraction of large polymers eluting between 6 and 9 min (Fig. 6b). As these higher molecular weight fractions consisted of glutenin polymers linked through disulfide bonds, this result was expected. However, even after reducing disulfide bonds and breaking non-covalent bonds, the gluten still contained the higher molecular weight fractions (F1 and F2), while zein was enriched in the lower molecular weight fractions (F3 and F4) (Fig. 6b). This is in line with the molecular weights reported for gluten (e.g. 30–60

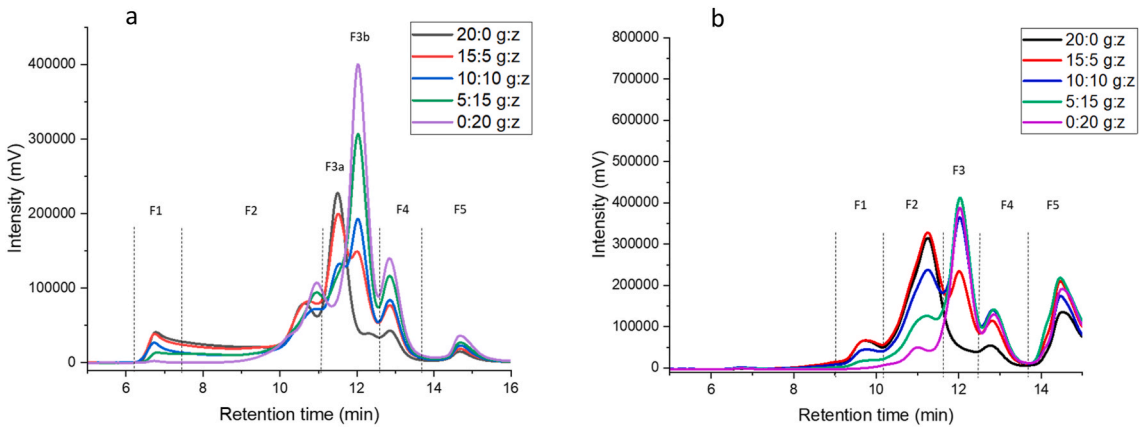

Fig. 6. Molecular weight distribution of proteins extracted from zein and/or gluten dough samples using SDS-containing buffer (a) and SDS-DTT-urea-containing buffer (b) analyzed by size exclusion chromatography (g:z stands for gluten:zein proportions).

kDa for LMW glutenin subunits and gliadin, and ~80 kDa for HMW glutenin subunits) and α-zein (19–22 kDa) (Delcour and Hoseney, 2010).

In addition, the 'theoretical' chromatograms of gluten-zein dough mixtures (15:5, 10:10, and 5:15 gluten:zein) were calculated based on the individual zein and gluten chromatograms and subsequently normalized to facilitate chromatogram comparisons (Fig. S8). For the 15:5 gluten:zein sample (Fig. S8a), with the chromatograms normalized on the (higher) left peak in the F3 fraction, higher peaks appeared for both higher molecular weight components (F1 and F2 fractions) and lower molecular weight components (right peak in F3 and F4) in the experimental data chromatograms relative to what the theoretically calculated chromatograms predicted. This may indicate that combining zein and gluten does lead relatively to some minor cross-linking between the proteins and also caused some de-aggregation. It is possible that the presence of zein hinders to some extent, gluten aggregation/network formation. The 10:10 gluten:zein sample chromatograms (normalized on the (higher) right peak in the F3 fraction) had a relatively higher fraction of the high molecular weight components (F1, F2 and F3) in the theoretically calculated chromatograms than experimental chromatograms (Fig. S8b). This seems to suggest that combining zein and gluten may alter the aggregation of the (gluten) proteins, hence, leading to a lower fraction of high molecular weight proteins (Fig. S8b). The experimental data chromatograms for 5:15 gluten:zein showed the same effect but much less outspoken (Fig. S8c).

4. Discussion

β-sheets are the dominant secondary structure in all studied dough samples. β-Sheet structures are stabilized by inter- or intramolecular hydrogen bonds and are usually found in the interior of folded protein molecules. This conformation facilitates embedding hydrophobic amino acids within the core of proteins (Wang et al., 2014). In addition, due to its relatively large surface area available for an ordered hydrogen bond formation, β-sheet structures may play an important part in the formation of protein fibrillar aggregates and have been reported to be the signature structural feature of protein fibrils (Erickson et al., 2012; Krebs et al., 2005; Pinotsi et al., 2016). It has been suggested that zein proteins tend to form insoluble β-sheet rich fibrils in a dough system which are responsible for the viscoelasticity of zein polymers (Chen et al., 2021; Erickson et al., 2012, 2020a; King et al., 2016; Taylor et al., 2013). The formation of fibrils by zein proteins in the here studied dough systems was supported by ThT fluorescence experiments. ThT fluorescence intensity increased with increasing zein concentration (Fig. 3c) and should be proportional to the concentration of bound ThT to fibrils and fibril length (Krebs et al., 2005). The results point to the presence of a higher structured fibrillar network with zein addition to the dough samples, providing more binding sites for ThT (Biancalana and Koide, 2010). The ThT fluorescence intensity has been reported to be positively correlated with the percentage of β-sheet secondary structure (Erickson et al., 2020a). The β-sheet structures in protein fibrils are likely interconnected and stabilized by a dense network of hydrogen bonds (Fig. 4c) (Pinotsi et al., 2016). The formation of these dense H-bonds was also supported by the fluorescence emission spectra of dough samples excited at 280 nm (Figs. 3b) and 350 nm (Fig. 3d), as explained in the *results* section. It has been reported that the formation of an extensive hydrogen bond network within β-sheet rich fibrils enables proton transfer and decreases electron excitation energy requirements resulting in intrinsic fluorescence emission (Pinotsi et al., 2016). The 0:20 gluten:zein samples showed a higher intensity at ~420 nm compared with 20:0 gluten:zein (Fig. 3d), further supporting the formation of more β-sheet rich fibrils in zein-rich dough samples. In addition, the length of zein fibrils clearly increased at higher zein concentration, according to SEM images (Fig. 5). We might not be able to directly relate the fibril formation by zein proteins to the fibril structures observed in SEM images, but these β-sheet rich fibrils may be a contributing factor to the increased length and diameter of the fibrils observed in the zein-rich dough samples (Fig. 5).

The cross-β-sheet structure in fibrils (Fig. 4c) consists of parallel and/or antiparallel β-sheets (Krebs et al., 2005). However, based on the presence of multiple antiparallel β-sheet peaks observed in FTIR and FT-Raman spectra of zein-rich dough samples (Figs. 1 and 2), we can assume that antiparallel β-sheet structures probably had a more prominent contribution to the cross-β-sheet architecture in fibrils formed by zein proteins (Fig. 4c). Hydrogen bonds in antiparallel β-sheets are slightly more stable than those in parallel β-sheets due to the more optimal (linear) hydrogen-bonding pattern. It is worth noting that hydrogen bonds are one of the main forces in zein network formation, while disulfide bonds seem to play a more important role in gluten network formation (Delcour et al., 2012).

Detailed analysis of IR and Raman spectra also showed the dominant presence of intermolecular β-sheets in gluten-rich dough samples, which decreased steadily upon addition of zein (Table 1). According to Zhou et al. (2014), increased water levels promote the formation of protein-water hydrogen bonds, leading to a simultaneous decrease in protein-protein interchain hydrogen bonds and, hence, intermolecular β-sheets in the gluten network. It can be assumed that the lower water-binding capacity of zein compared with gluten resulted in more available water in the gluten-zein dough samples. This would have promoted the formation of more water-protein hydrogen bonds and decreased the intermolecular β-sheet content. Intramolecular β-sheets are likely less affected by the higher level of free water as the hydrophobic cores of intramolecular β-sheets are less accessible for water. The presence of more available water in zein-dominated dough samples was

further supported by the significantly ($p < 0.05$) higher syneresis values of the 0:20 gluten:zein sample (3%) compared to the syneresis of the 20:0 gluten:zein sample (0%) (Fig. S9). The higher water availability in the zein-rich dough samples may also have resulted in a red-shifted Trp emission in the fluorescence spectra of dough samples (Fig. 3a, Table S1), likely indicating the exposure of Trp residues to a more hydrophilic environment. In polar solvents, the fluorescence emission of a single fully solvent-exposed Trp molecule typically exhibits a bathochromic or red-shift, while, in nonpolar environments the Trp fluorescence emission typically exhibits a hypsochromic or blue-shift (Fig. 4a) (Bonomi et al., 2004; Lakowicz, 2013). In this study, gluten was the only protein-containing Trp as zein is Trp-deficient. The results suggest that the Trp residues were increasingly exposed to a more hydrophilic environment when more zein was included in the protein fraction. There could indeed be more free water available for gluten (Trp) in samples with higher zein contents due to the higher hydrophobicity of zein and its lower water-binding capacity relative to gluten (Shukla and Cheryan, 2001). However, the Trp emission signal that is measured is a cumulative signal of different Trp residues present in different environments in the complex sample, and caution has to be taken not to enroll in overinterpretation of these data. In addition to the effect of higher water availability on intermolecular β-sheet structure content, zein lacks the proteins and protein analogues that are at the basis of the intermolecular β-sheet structures in gluten, *i.e.,* the HMW glutenin subunits (Mejia et al., 2007). This could be another factor limiting 'zein's propensity to form intermolecular β-sheets.

While disulfide bridges play a crucial role in the formation of a gluten network (Nawrocka et al., 2017), they are likely less critical in zein network formation due to the low number of cysteine residues in this protein (Delcour and Hoseney, 2010). This is supported by HPLC results where similar chromatograms were observed for zein-only samples with and without DTT (Fig. S10a), while gluten showed a different profile under reduced and non-reduced conditions (Fig. S10b). Hydrogen bonds and the hydrophobic effect are the main drivers in the formation of zein's viscoelastic state (Delcour and Hoseney, 2010). The analysis of the disulfide region (490-550 cm^{-1}) showed that the majority of disulfide bonds in the 20:0 gluten:zein samples are in the g-g-g conformation (Table 2). The majority of the cystine linkages in proteins are reportedly in this most stable g-g-g conformation. Stable disulfide bridges are crucial to the stability of the gluten protein network (Zhou et al., 2014). Addition of zein to the dough system considerably increased the amount of t-g-t conformation at the expense of g-g-g conformation (Table 2). According to Zhou et al. (2014), protein water absorption is directly related to the formation of the stable disulfide bond conformation (g-g-g). Under high hydration levels, disulfide bridges tend to adopt a g-g-g conformation (Nawrocka et al., 2017). The syneresis experiment (Fig. S9) and previous research (Delcour and Hoseney, 2010) already pointed to the inferior water-binding capacity of zein. Cysteine residues in zein will most probably, in line with the more hydrophobic nature of this protein, be less hydrated, which could explain that the disulfide bonds in zein samples tend to adopt the less stable t-g-t conformation. The decrease in the number of g-g-g conformation upon addition of zein can also be due to the displacement/disruption of gluten polypeptide chains as a result of zein addition (Zhou et al., 2014). The SE-HPLC results also showed a potential effect of zein on gluten aggregation (Fig. S8).

The fluorescence spectra of zein-containing dough samples consistently included a Tyr peak (305–330 nm), even in those samples containing 15:5 gluten:zein (Fig. 3b. In the 20:0 gluten-zein samples, however, very efficient Tyr fluorescence quenching occurs through Trp as no Tyr peak is seen in the spectra of these samples (Fig. 3b). In addition, the proportion of Tyr:Trp in the protein fraction of dough samples increases with increasing zein content which will result in a more prominent Tyr signal in zein-rich samples. These data might suggest that two distinct network structures composed of gluten and zein are formed, which is in line with CLSM results by Bugusu et al. (2002). The SE-HPLC results (Fig. S8) also showed no significant aggregation occurred in the dough system by mixing zein and gluten proteins which supports the idea that these two proteins probably did not significantly interact or mix with each other. Quite conversely, the addition of zein to gluten dough seemed to rather decrease protein aggregation. In addition, FT-Raman results showed that the I_{850}/I_{830} value in the samples containing zein is smaller than 1, suggesting that zein contains more buried Tyr residues compared to gluten. The seemingly more water-exposed (surface-positioned) gluten Trp residues and more buried, less hydrated zein Tyr residues in gluten-zein dough samples support that these residues are not in close proximity of each other. The higher values of the Tyr doublet in the Raman spectra in the 20:0 gluten: zein dough sample indicate that the hydrogen bonds in which the Tyr OH groups are involved in the gluten samples are stronger than those found in the zein network. This is in line with the higher amount of strong hydrogen-bonded intermolecular β-sheet structures in gluten (Table 1). This I_{850}/I_{830} value suggests the exposure of gluten Tyr residues (alongside the Trp residues) at the protein surface and their possible involvement in the formation of intermolecular hydrogen-bonded β-sheet structures (Rumińska et al., 2020).

By adding zein to the system, a decrease in intermolecular β-sheet structures has been observed (Table 1), and a more unordered conformation of the protein network is anticipated. This is consistent with the obtained SEM images in which the continuity of the film-like gluten network was disrupted by the incorporation of zein into the dough system (Fig. 5). This results in a less compact gluten structure, a hypothesis also supported by the decrease in intermolecular β-sheet structures upon addition of zein to the dough systems. The disruption of the compact gluten network upon adding zein to the system is also in line with all the analysis results pointing to more (gluten exposure to) free water in the system.

It has been shown that zein forms fibrillar protein aggregates in its viscoelastic dough state (Erickson et al., 2012; Guo et al., 2005; Ncube et al., 2022). The mechanism for zein's fibrillation and aggregation behavior is not completely understood at present, but it seems to be incompatible with the gluten aggregation behavior. The higher hydrophobicity of zein compared with gluten seems to be a driving factor for enhanced interactions among these molecules to form of fibrils (Ncube et al., 2022). Self-assembly of β-sheet rich fibrils is one of the models proposed to explain zein's aggregation behavior (Chen et al., 2021; Erickson et al., 2012). These β-sheet rich fibrils (Erickson et al., 2012) can be used as the basis for the development of viscoelastic aggregates in zein-containing dough samples. However, the gas retention capacity of these fibrils should be further investigated as they might not have the same ability as the film structures observed for gluten proteins.

5. Conclusions

The present study provides complementary submolecular, molecular, supramolecular, and microstructural information on dough structures made with zein and gluten proteins. Zein, with its lower water-binding capacity, may increase the available water content in the dough samples, creating a more hydrophilic environment for the gluten proteins, leading to a weakening of the intermolecular β-sheet structure, increased exposure of cystine, Trp, and Tyr residues to water, and more pronounced syneresis of the zein-containing dough samples. Furthermore, zein and gluten do not seem to interact tightly with each other. The formation of two 'separate' protein network structures is likely and supported by Tyr quenching experiments, SEM analysis, and SE-HPLC results. Zein is known to form more fibrillar structures, while gluten upon hydration and shear forms film-like structures. The nature of the formed gluten-zein protein network and hypothesized protein incompatibility upon dough formation requires further investigation. However, the obtained information in this study demonstrated the suitability and complementarity of spectroscopy techniques to study complex cereal systems in a non-invasive way.

CRediT authorship contribution statement

Azin Sadat: Conceptualization, Methodology, Validation, Formal analysis, Investigation, Writing – original draft, Visualization. **Maria G. Corradini:** Conceptualization, Methodology, Formal analysis, Resources, Writing – review & editing, Supervision. **Iris J. Joye:** Conceptualization, Formal analysis, Resources, Writing – review & editing, Supervision, Funding acquisition.

Declaration of competing interest

The authors declare the following financial interests/personal relationships which may be considered as potential competing interests: Dr. Maria G. Corradini is the Associate Editor of the Current Research in Food Science journal. Given her role as Associate Editor at the time of submission, Maria G. Corradini had no involvement in the peer review of this article and had no access to information regarding its peer review. Full responsibility for the editorial process for this article was delegated to another editor, as per the Journal guidelines.

Acknowledgments

Azin Sadat wishes to acknowledge the Ontario Trillium Scholarship for funding her project. Iris J. Joye and Maria G. Corradini acknowledge NSERC (Discovery Grant Program) for providing research funding. The authors would like to thank Dr. Leonid Brown for providing the FT-Raman facility and Dr. Fernanda Peyronel for providing technical assistance in SEM measurements. The authors would like also to thank Mr. Louis A. Colaruotolo's contribution to the identification of the 440 nm fluorescence emission band.

Appendix A. Supplementary data

Supplementary data to this article can be found online at https://doi.org/10.1016/j.crfs.2022.02.009.

References

Alhusein, N., Blagbrough, I.S., Paul, A., 2013. Zein/polycaprolactone electrospun matrices for localised controlled delivery of tetracycline. Drug Deliv. Transl. Res. 3 (6), 542–550.
An, B., Wu, X., Li, M., Chen, Y., Li, F., Yan, X., Wang, J., Li, C., Brennan, C., 2016. Hydrophobicity-modulating self-assembled morphologies of α-zein in aqueous ethanol. Int. J. Food Sci. Technol. 51 (12), 2621–2629.
Andersen, C.M., Mortensen, G., 2008. Fluorescence spectroscopy: a rapid tool for analyzing dairy products. J. Agric. Food Chem. 56 (3), 720–729.
Andersson, H., Öhgren, C., Johansson, D., Kniola, M., Stading, M., 2011. Extensional flow, viscoelasticity and baking performance of gluten-free zein-starch doughs supplemented with hydrocolloids. Food Hydrocolloids 25 (6), 1587–1595.
Argos, P., Pedersen, K., Marks, M.D., Larkins, B.A., 1982. A structural model for maize zein proteins. J. Biol. Chem. 257 (17), 9984–9990.
Bache, I.C., Donald, A.M., 1998. The structure of the gluten network in dough: a study using environmental scanning electron microscopy. J. Cereal. Sci. 28 (2), 127–133.
Bagagli, M.P., Jazaeri, S., Bock, J.E., Seetharaman, K., Sato, H.H., 2014. Effect of transglutaminase, citrate buffer, and temperature on a soft wheat flour dough system. Cereal Chem. 91 (5), 460–465.
Belton, P.S., Colquhoun, I.J., Grant, A., Wellner, N., Field, J.M., Shewry, P.R., Tatham, A. S., 1995. FTIR and NMR studies on the hydration of a high-Mr subunit of glutenin. Int. J. Biol. Macromol. 17 (2), 74–80.
Biancalana, M., Koide, S., 2010. Molecular mechanism of Thioflavin-T binding to amyloid fibrils. Biochim. Biophys. Acta Protein Proteonomics 1804 (7), 1405–1412.
Bock, J.E., Connelly, R.K., Damodaran, S., 2013. Impact of bran addition on water properties and gluten secondary structure in wheat flour doughs studied by attenuated total reflectance Fourier transform infrared spectroscopy. Cereal Chem. 90 (4), 377–386.
Bock, J.E., Damodaran, S., 2013. Bran-induced changes in water structure and gluten conformation in model gluten dough studied by Fourier transform infrared spectroscopy. Food Hydrocolloids 31 (2), 146–155.
Bonomi, F., Mora, G., Pagani, M.A., Iametti, S., 2004. Probing structural features of water-insoluble proteins by front-face fluorescence. Anal. Biochem. 329 (1), 104–111.
Bugusu, B.A., Campanella, O., Hamaker, B.R., 2001. Improvement of sorghum-wheat composite dough rheological properties and breadmaking quality through zein addition. Cereal Chem. 78 (1), 31–35.
Bugusu, B.A., Hamaker, B.R., Rajwa, B., 2002. Interaction of maize zein with wheat gluten in composite dough and bread as determined by confocal laser scanning microscopy. Scanning: J. Scanning Microsc. 24 (1), 1–5.
Cao, W., Pink, D.A., Joye, I.J., 2021. Effect of low ion concentrations on thiol oxidation rates, protein crosslinking, water mobility and rheology of hard wheat flour dough. J. Cereal. Sci. 99, 103204 https://doi.org/10.1016/J.JCS.2021.103204.
Cebi, N., Dogan, C.E., Develioglu, A., Yayla, M.E.A., Sagdic, O., 2017. Detection of l-cysteine in wheat flour by Raman microspectroscopy combined chemometrics of HCA and PCA. Food Chem. 228, 116–124.
Cerf, E., Sarroukh, R., Tamamizu-Kato, S., Breydo, L., Derclaye, S., Dufrêne, Y.F., Narayanaswami, V., Goormaghtigh, E., Ruysschaert, J.-M., Raussens, V., 2009. Antiparallel β-sheet: a signature structure of the oligomeric amyloid β-peptide. Biochem. J. 421 (3), 415–423.
Chen, D., Jones, O.G., Campanella, O.H., 2021. Plant protein-based fibers: fabrication, characterization, and potential food applications. Crit. Rev. Food Sci. Nutr. 1–25.
Chen, L., Subirade, M., 2009. Elaboration and characterization of soy/zein protein microspheres for controlled nutraceutical delivery. Biomacromolecules 10 (12), 3327–3334.
Chen, Y., Ye, R., Liu, J., 2014. Effects of different concentrations of ethanol and isopropanol on physicochemical properties of zein-based films. Ind. Crop. Prod. 53, 140–147.
Delcour, J.A., Hoseney, R.C., 2010. Principles of Cereal Science and Technology. AACC International. *Inc.*, St. Paul, MN, USA, pp. 229–235.
Delcour, J.A., Joye, I.J., Pareyt, B., Wilderjans, E., Brijs, K., Lagrain, B., 2012. Wheat gluten functionality as a quality determinant in cereal-based food products. Annu. Rev. Food Sci. Technol. 3, 469–492.
Erickson, D.P., Campanella, O.H., Hamaker, B.R., 2012. Functionalizing maize zein in viscoelastic dough systems through fibrous, β-sheet-rich protein networks: an alternative, physicochemical approach to gluten-free breadmaking. Trends Food Sci. Technol. 24 (2), 74–81.
Erickson, D.P., Ozturk, O.K., Selling, G., Chen, F., Campanella, O.H., Hamaker, B.R., 2020a. Corn zein undergoes conformational changes to higher β-sheet content during its self-assembly in an increasingly hydrophilic solvent. Int. J. Biol. Macromol. 157, 232–239.
Erickson, D.P., Ozturk, O.K., Selling, G., Chen, F., Campanella, O.H., Hamaker, B.R., 2020b. Corn zein undergoes conformational changes to higher β-sheet content during its self-assembly in an increasingly hydrophilic solvent. Int. J. Biol. Macromol. 157, 232–239.
Escamilla-García, M., Calderon-Dominguez, G., Chanona-Perez, J.J., Farrera-Rebollo, R. R., Andraca-Adame, J.A., Arzate-Vazquez, I., Mendez-Mendez, J.V., Moreno-Ruiz, L. A., 2013. Physical and structural characterisation of zein and chitosan edible films using nanotechnology tools. Int. J. Biol. Macromol. 61, 196–203.
Farrokhi, F., Badii, F., Ehsani, M.R., Hashemi, M., 2019. Functional and thermal properties of nanofibrillated whey protein isolate as functions of denaturation temperature and solution pH. Colloids Surf. A Physicochem. Eng. Asp. 583, 124002.
Federici, E., Selling, G.W., Campanella, O.H., Jones, O.G., 2020. Incorporation of plasticizers and Co-proteins in zein electrospun fibers. J. Agric. Food Chem. 68 (49), 14610–14619.
Federici, E., Selling, G.W., Campanella, O.H., Jones, O.G., 2021. Thermal treatment of dry zein to improve rheological properties in gluten-free dough. Food Hydrocolloids 115, 106629.
Fernandez, A., Torres-Giner, S., Lagaron, J.M., 2009. Novel route to stabilization of bioactive antioxidants by encapsulation in electrospun fibers of zein prolamine. Food Hydrocolloids 23 (5), 1427–1432.
Ferrer, E.G., Gómez, A.V., Añón, M.C., Puppo, M.C., 2011. Structural changes in gluten protein structure after addition of emulsifier. A Raman spectroscopy study. Spectrochim. Acta Mol. Biomol. Spectrosc. 79 (1), 278–281.
Gao, J., Koh, A.H.S., Tay, S.L., Zhou, W., 2017. Dough and bread made from high-and low-protein flours by vacuum mixing: Part 1: gluten network formation. J. Cereal. Sci. 74, 288–295.
Guo, Y., Liu, Z., An, H., Li, M., Hu, J., 2005. Nano-structure and properties of maize zein studied by atomic force microscopy. J. Cereal. Sci. 41 (3), 277–281.
Hoseney, R.C., 1986. Principles of Cereal Science and Technology.
Hu, K., Huang, X., Gao, Y., Huang, X., Xiao, H., McClements, D.J., 2015. Core–shell biopolymer nanoparticle delivery systems: synthesis and characterization of curcumin fortified zein–pectin nanoparticles. Food Chem. 182, 275–281.
Jazaeri, S., Bock, J.E., Bagagli, M.P., Iametti, S., Bonomi, F., Seetharaman, K., 2015. Structural modifications of gluten proteins in strong and weak wheat dough during mixing. Cereal Chem. 92 (1), 105–113.
Johansson, D., Krona, A., Stading, M., 2012. Influence of surface lipids in commercial zein on microstructure and rheological properties of gluten-free dough. Annu. Trans. Nordic Rheol. Soc. 20, 247–251.
Khuzwayo, T.A., Taylor, J.R.N., Taylor, J., 2020. Influence of dough sheeting, flour pre-gelatinization and zein inclusion on maize bread dough functionality. LWT 121, 108993.
King, B.L., Taylor, J., Taylor, J.R.N., 2016. Formation of a viscoelastic dough from isolated total zein (α-, β-and γ-zein) using a glacial acetic acid treatment. J. Cereal. Sci. 71, 250–257.
Kokawa, M., Fujita, K., Sugiyama, J., Tsuta, M., Shibata, M., Araki, T., Nabetani, H., 2011. Visualization of gluten and starch distributions in dough by fluorescence fingerprint imaging. Biosci. Biotechnol. Biochem. 75 (11), 2112–2118.
Krebs, M.R.H., Bromley, E.H.C., Donald, A.M., 2005. The binding of thioflavin-T to amyloid fibrils: localisation and implications. J. Struct. Biol. 149 (1), 30–37.
Lakowicz, J.R., 2013. Principles of Fluorescence Spectroscopy. Springer Science & Business Media.
Lawton, J.W., 1992. Viscoelasticity of zein-starch doughs. Cereal Chem. 69 (4), 351–355.

Mejia, C.D., Mauer, L.J., Hamaker, B.R., 2007. Similarities and differences in secondary structure of viscoelastic polymers of maize α-zein and wheat gluten proteins. J. Cereal. Sci. 45 (3), 353–359.
Nawrocka, A., Miś, A., Szymańska-Chargot, M., 2016a. Characteristics of relationships between structure of gluten proteins and dough rheology–influence of dietary fibres studied by FT-Raman spectroscopy. Food Biophys. 11 (1), 81–90.
Nawrocka, A., Szymańska-Chargot, M., Miś, A., Kowalski, R., Gruszecki, W.I., 2016b. Raman studies of gluten proteins aggregation induced by dietary fibres. Food Chem. 194, 86–94.
Nawrocka, A., Szymańska-Chargot, M., Miś, A., Ptaszyńska, A.A., Kowalski, R., Waśko, P., Gruszecki, W.I., 2015. Influence of dietary fibre on gluten proteins structure–a study on model flour with application of FT-Raman spectroscopy. J. Raman Spectrosc. 46 (3), 309–316.
Nawrocka, A., Szymańska-Chargot, M., Miś, A., Wilczewska, A.Z., Markiewicz, K.H., 2016c. Dietary fiber-induced changes in the structure and thermal properties of gluten proteins studied by Fourier transform-Raman spectroscopy and thermogravimetry. J. Agric. Food Chem. 64 (10), 2094–2104.
Nawrocka, A., Szymańska-Chargot, M., Miś, A., Wilczewska, A.Z., Markiewicz, K.H., 2017. Effect of dietary fibre polysaccharides on structure and thermal properties of gluten proteins–A study on gluten dough with application of FT-Raman spectroscopy, TGA and DSC. Food Hydrocolloids 69, 410–421.
Ncube, M.B., Taylor, J., Bean, S.R., Ioerger, B.P., Taylor, J.R.N., 2022. Modification of zein dough functionality using kafirin as a coprotein. Food Chem. 373, 131547.
Pfeuti, G., Longstaffe, J., Brown, L.S., Shoveller, A.K., Taylor, C.M., Bureau, D.P., 2019. Disulphide bonds and cross-linked amino acids may affect amino acid utilization in feather meal fed to rainbow trout (Oncorhynchus mykiss). Aquacult. Res. 50 (8), 2081–2095.
Piccirilli, F., Schirò, G., Vetri, V., Lupi, S., Perucchi, A., Militello, V., 2015. Decoding vibrational states of Concanavalin A amyloid fibrils. Biophys. Chem. 199, 17–24.
Pinotsi, D., Grisanti, L., Mahou, P., Gebauer, R., Kaminski, C.F., Hassanali, A., Kaminski Schierle, G.S., 2016. Proton transfer and structure-specific fluorescence in hydrogen bond-rich protein structures. J. Am. Chem. Soc. 138 (9), 3046–3057.
Piot, O., Autran, J.-C., Manfait, M., 2001. Investigation by confocal Raman microspectroscopy of the molecular factors responsible for grain cohesion in thetriticum aestivum bread wheat. Role of the cell walls in the starchy endosperm. J. Cereal. Sci. 34 (2), 191–205.
Prestrelski, S.J., Tedeschi, N., Arakawa, T., Carpenter, J.F., 1993. Dehydration-induced conformational transitions in proteins and their inhibition by stabilizers. Biophys. J. 65 (2), 661–671.
Rombouts, I., Jansens, K.J.A., Lagrain, B., Delcour, J.A., Zhu, K.-X., 2014. The impact of salt and alkali on gluten polymerization and quality of fresh wheat noodles. J. Cereal. Sci. 60 (3), 507–513.
Rumińska, W., Szymańska-Chargot, M., Wiącek, D., Sobota, A., Markiewicz, K.H., Wilczewska, A.Z., Miś, A., Nawrocka, A., 2020. FT-Raman and FT-IR studies of the gluten structure as a result of model dough supplementation with chosen oil pomaces. J. Cereal. Sci., 102961
Sadat, A., Corradini, M.G., Joye, I.J., 2019. Molecular spectroscopy to assess protein structures within cereal systems. Curr. Opin. Food Sci. 25, 42–51.
Sadat, A., Joye, I.J., 2020. Peak fitting applied to fourier transform infrared and Raman spectroscopic analysis of proteins. Appl. Sci. 10 (17), 5918.
Schober, T.J., Bean, S.R., Boyle, D.L., Park, S.-H., 2008. Improved viscoelastic zein–starch doughs for leavened gluten-free breads: their rheology and microstructure. J. Cereal. Sci. 48 (3), 755–767.
Schober, T.J., Moreau, R.A., Bean, S.R., Boyle, D.L., 2010. Removal of surface lipids improves the functionality of commercial zein in viscoelastic zein-starch dough for gluten-free breadmaking. J. Cereal. Sci. 52 (3), 417–425.
Sen, P., Fatima, S., Ahmad, B., Khan, R.H., 2009. Interactions of thioflavin T with serum albumins: spectroscopic analyses. Spectrochim. Acta Mol. Biomol. Spectrosc. 74 (1), 94–99.
Shukla, R., Cheryan, M., 2001. Zein: the industrial protein from corn. Ind. Crop. Prod. 13 (3), 171–192.
Sly, A.C., Taylor, J., Taylor, J.R.N., 2014. Improvement of zein dough characteristics using dilute organic acids. J. Cereal. Sci. 60 (1), 157–163.
Smith, B.M., Bean, S.R., Selling, G., Sessa, D., Aramouni, F.M., 2014. Role of non-covalent interactions in the production of visco-elastic material from zein. Food Chem. 147, 230–238.
Taylor, J., Anyango, J.O., Taylor, J.R.N., 2013. Developments in the science of zein, kafirin, and gluten protein bioplastic materials. Cereal Chem. 90 (4), 344–357.
Wang, Y., Su, C.-P., Schulmerich, M., Padua, G.W., 2013. Characterization of core–shell structures formed by zein. Food Hydrocolloids 30 (2), 487–494.
Wang, Z., Li, Y., Jiang, L., Qi, B., Zhou, L., 2014. Relationship between secondary structure and surface hydrophobicity of soybean protein isolate subjected to heat treatment. J. Chem. 2014.
Wellner, N., Mills, E.N.C., Brownsey, G., Wilson, R.H., Brown, N., Freeman, J., Halford, N.G., Shewry, P.R., Belton, P.S., 2005. Changes in protein secondary structure during gluten deformation studied by dynamic Fourier transform infrared spectroscopy. Biomacromolecules 6 (1), 255–261.
Wheelwright, W.V.K., Easteal, A.J., Ray, S., Nieuwoudt, M.K., 2013. A one-step approach for esterification of zein with methanol. J. Appl. Polym. Sci. 127 (5), 3500–3505.
Yada, R.Y., Jackman, R.L., 2012. Protein Structure-Function Relationships in Foods. Springer Science & Business Media.
Zhang, B., Luo, Y., Wang, Q., 2010. Development of silver– zein composites as a promising antimicrobial agent. Biomacromolecules 11 (9), 2366–2375.
Zhou, Y., Zhao, D., Foster, T.J., Liu, Y., Wang, Y., Nirasawa, S., Tatsumi, E., Cheng, Y., 2014. Konjac glucomannan-induced changes in thiol/disulphide exchange and gluten conformation upon dough mixing. Food Chem. 143, 163–169.